Institution of MECHANICAL ENGINEERS

Journal of AEROSPACE ENGINEERING

Original Article

Proc IMechE Part G:
J Aerospace Engineering
0(0) 1–11

DOI: 10.1177/0954410020920040
journals.sagepub.com/home/pig
SAGE

Initial design of low-thrust trajectories based on the Bezier curve-based shaping approach

Zichen Fan, Mingying Huo, Naiming Qi, Ce Zhao, Ze Yu and Tong Lin

Abstract

This paper presents a method to use the Bezier curve to rapidly generate three-dimensional low-thrust trajectories, which can provide a suitable initial approximation to be used for more accurate trajectory optimal control tools. Two missions, from Earth to Mars and the asteroid Dionysus, are considered to evaluate the performance of the method. In order to verify the advantages of this method, it is compared with the finite Fourier series method. Numerical results show that the Bezier method can get better performance index in shorter computation time compared with the finite Fourier series method. The applicability of the solution obtained by Bezier method is evaluated by introducing the obtained solution into the Gauss pseudospectral method as an initial guess. The simulation results show that the Bezier method can rapidly generate a very suitable three-dimensional initial trajectory for the optimal solver. This is very important for rapid evaluation of the feasibility of a large number of low-thrust flight schemes in the preliminary mission design stage.

Keywords

Preliminary mission analysis, low-thrust trajectory approximation, Bezier method, shape-based, fast computation

Date received: 29 September 2019; accepted: 13 March 2020

Introduction

With the development of low-thrust propulsion systems,[1–6] for the optimal trajectory design problem, the design variables gradually change from finite to infinite.[7,8] Low-thrust mission design[9–12] requires a method to approximate the trajectory and mission cost, which are very important.[13,14] In the design of a transfer trajectory, boundary conditions (BCs) and equations of motion (EoM) need to be satisfied, which makes the low-thrust mission design more challenging both mathematically and computationally.[15,16] For this problem, both indirect and direct optimization methods require a very suitable initial solution and are usually computationally demanding, which excludes the possibility of rapid feasibility assessments of a large number of low-thrust flight schemes in the preliminary mission design stage. Hence, rapid initial trajectory design is of great significance for trajectory optimization and mission analysis.

In recent years, shape-based (SB) methods have been proposed for rapid trajectory generation.[17,18] Petropoulos and Longuski[17] proposed the first SB method, who used the exponential sinusoid function to describe the trajectory. After that, many researchers, such as Pascale and Vasile,[19] Wall and Conway and Wall,[20,21] Xie et al.,[22,23] Novak and Vasile,[15] Gondelach and Noomen,[24] Zeng et al.,[25] and Peloni et al.[26] put forward many SB methods. Recently, Taheri and Abdelkhalik[7,27,28] put forward a flexible method based on the FFS approximation of the trajectory shape. Furthermore, Taheri et al.[29] described the trajectory in spherical coordinate system by the FFS method. Recently, Huo et al.[30] used the FFS method and Bezier curves[31] to design the 3D trajectories of electric solar wind sail.[32]

This paper takes advantage of the Bezier curve to rapidly design the 3D low-thrust trajectory. For the rendezvous problem, BCs can be satisfied simultaneously by computing 12 coefficients in the Bezier curve function. When Bezier orders of coordinate approximations are three, the transfer trajectory is determined analytically by BCs, and there is no

School of Astronautics, Harbin Institute of Technology, Harbin, China

Corresponding author:
Mingying Huo, School of Astronautics, Harbin Institute of Technology, Harbin 150001, China.
Email: huomingying@hit.edu.cn

unknown coefficient to be optimized.[31] If Bezier orders are greater than three, the transfer trajectory cannot only be determined analytically by BCs. There are unknown coefficients to be optimized to satisfy certain thrust constraints. This feature is similar to FFS method.[28] For the time-fixed transfer problem, both the matrices in the Bezier and FFS methods are constant matrices. However, for the time-free transfer problem, some of the matrices in the FFS method need to be calculated within each iteration, which leads to the faster computation speed of the Bezier method than the FFS method. Therefore, this paper verifies the effectiveness of the Bezier method through comparison with FFS. The applicability of the solution obtained by Bezier method is evaluated by introducing the obtained solution into the GPM as an initial guess.

This paper is organized as follows. The next section introduces the coordinate systems, EoM, and BCs. Then, the Bezier method is applied to generate the approximated transfer trajectory. In the subsequent section, the effectiveness of the Bezier method is checked by the simulation of Earth-Mars and Earth-Dionysus rendezvous missions, through comparison with FFS and GPM. Finally, the conclusion is given in the last section.

Problem description

As shown in Figure 1, introduce a cylindrical coordinate system where r, θ, and z are the radial distance, the azimuth angle and the altitude of the spacecraft, respectively.

The EoM written in the cylindrical coordinate system are[28]

$$\begin{aligned} &\ddot{r} - r\dot{\theta}^2 + \mu_{\odot} r/s^3 = a_r \\ &r\ddot{\theta} + 2\dot{r}\dot{\theta} = a_\theta \\ &\ddot{z} + \mu_{\odot} z/s^3 = a_z \end{aligned} \tag{1}$$

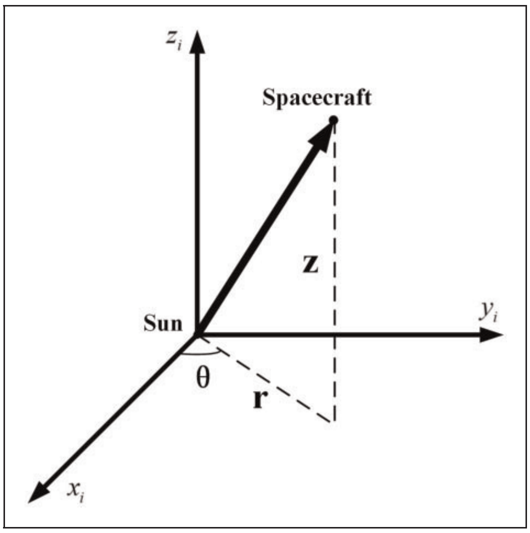

Figure 1. Cylindrical coordinates.

where $s = \sqrt{r^2 + z^2}$ is the distance between the center of the spacecraft and the central body (the Sun), $\mu_{\odot}$ is the gravitational parameter of the Sun, while a_r, a_θ, and a_z are the components of the propulsive acceleration. Therefore, the required propulsive acceleration, a, is

$$a = \sqrt{a_r^2 + a_\theta^2 + a_z^2} \tag{2}$$

The total velocity variation ΔV can be obtained by computing the following integral, which is the performance index to be minimized

$$\Delta V = \int_0^T a \mathrm{d}t \tag{3}$$

where T is the total flight time.

In a general 3D rendezvous problem, the following 12 initial and final BCs need to be satisfied

$$\begin{aligned} &r(\tau = 0) = r_i,\ r(\tau = 1) = r_f,\ r'(\tau = 0) = T\dot{r}_i, \\ &r'(\tau = 1) = T\dot{r}_f \\ &\theta(\tau = 0) = \theta_i,\ \theta(\tau = 1) = \theta_f,\ \theta'(\tau = 0) = T\dot{\theta}_i, \\ &\theta'(\tau = 1) = T\dot{\theta}_f \\ &z(\tau = 0) = z_i,\ z(\tau = 1) = z_f,\ z'(\tau = 0) = T\dot{z}_i, \\ &z'(\tau = 1) = T\dot{z}_f \end{aligned} \tag{4}$$

where the subscript "i" denotes the initial condition, and the subscript "f" denotes the final condition. $0 \leqslant \tau = t/T \leqslant 1$ is the scaled time, and t is the current flight time. The symbol $\cdot$ and the superscript $'$ denote the derivative with respect to t and τ, respectively.

For the calculation of the number of revolutions of spacecraft, it can be set as a fixed value, or it can be calculated automatically through iteration. If it is calculated automatically through iteration, its calculation is determined by the starting point, arrival point, and transfer time. The calculation equation is as follows

$$N_{rev} = (\theta_i + 0.5(\dot{\theta}_i + \dot{\theta}_f)T - \theta_f)/(2 * \pi) \tag{5}$$

Then round the calculation result to obtain the number of revolutions.

Bezier shape-based method

States approximation

According to Huo et al.,[31] in the Bezier method, r is expanded in the following form (θ and z have similar forms)

$$r(\tau) = \sum_{j=0}^{n_r} B_{r,j}(\tau) P_{r,j} \tag{6}$$

where n_r is the order of Bezier curve function, $P_{r,j}$ are the unknown Bezier coefficients, and $B_{r,j}(\tau)$ are the Bezier basis functions of the state variables, that is

$$B_{r,j}(\tau) = \frac{n_r!}{j!(n_r - j)!}\tau^j (1-\tau)^{n_r - j} \quad j \in [0, n_r] \tag{7}$$

According to equation (5), the first-order and second-order τ-derivatives of r can be obtained as follows

$$r'(\tau) = \sum_{j=0}^{n_r} B'_{r,j}(\tau)P_{r,j} \quad r''(\tau) = \sum_{j=0}^{n_r} B''_{r,j}(\tau)P_{r,j} \tag{8}$$

where $B'_{r,j}(\tau)$ and $B''_{r,j}(\tau)$ are the first-order and second-order τ-derivatives of the Bezier basis functions of the state variables, respectively (see Huo et al.[31] for details).

By substituting $\tau = 0$ and $\tau = 1$ into equation (6), we can find the characteristics of the Bezier basis functions at the boundaries

$$\begin{aligned}
B_{r,j}(\tau = 0) &= \begin{cases} 1 & j = 0 \\ 0 & j \in [1, n_r] \end{cases} \\
B_{r,j}(\tau = 1) &= \begin{cases} 0 & j \in [0, n_r - 1] \\ 1 & j = n_r \end{cases} \\
B'_{r,j}(\tau = 0) &= \begin{cases} -n_r & j = 0 \\ n_r & j = 1 \\ 0 & j \in [2, n_r] \end{cases} \\
B'_{r,j}(\tau = 1) &= \begin{cases} 0 & j \in [0, n_r - 2] \\ -n_r & j = n_r - 1 \\ n_r & j = n_r \end{cases}
\end{aligned} \tag{9}$$

Considering the approximation functions (equations (5) and (7)) and BCs (equation (4)), we can obtain the following equations

$$\begin{aligned}
r_i &= r(\tau = 0) = P_{r,0} \\
r_f &= r(\tau = 1) = P_{r,n_r} \\
T\dot{r}_i &= r'(\tau = 0) = n_r(P_{r,1} - P_{r,0}) \\
T\dot{r}_f &= r'(\tau = 1) = n_r(P_{r,n_r} - P_{r,n_r-1})
\end{aligned} \tag{10}$$

Consequently, the four Bezier coefficients $P_{r,0}$, $P_{r,1}$, P_{r,n_r-1}, and P_{r,n_r} can be determined by BCs

$$\begin{aligned}
P_{r,0} &= r_i & P_{r,1} &= r_i + T\dot{r}_i/n_r \\
P_{r,n_r-1} &= r_f - T\dot{r}_f/n_r & P_{r,n_r} &= r_f
\end{aligned} \tag{11}$$

Unlike Taheri and Abdelkhalik,[28] in this paper, only equation (11) needs to be repeatedly calculated, so the overall computation time of this method is shorter.

The general problem is to find a feasible flight trajectory using a low-thrust propulsion system. In order to impose enough constraints on the low-thrust acceleration along the trajectory, some discrete points need to be evaluated. The Legendre-Gauss distribution of discrete points is adopted, which are the roots of the mth-degree Legendre polynomial

$$\tau_1 = 0 < \tau_2 < \cdots < \tau_{m-1} < \tau_m = 1 \tag{12}$$

Since the scaled-time vector is written as a column vector, r and its associated first and second τ-derivatives can be written in matrix form as

$$\begin{aligned}
[r]_{m\times 1} &= [B_r]_{m\times(n_r+1)}[P_r]_{(n_r+1)\times 1} \\
[r']_{m\times 1} &= [B'_r]_{m\times(n_r+1)}[P_r]_{(n_r+1)\times 1} \\
[r'']_{m\times 1} &= [B''_r]_{m\times(n_r+1)}[P_r]_{(n_r+1)\times 1}
\end{aligned} \tag{13}$$

where $[P_r] = \begin{bmatrix} P_{r,0} & P_{r,1} & [X_r]^T_{(n_r-3)\times 1} & P_{r,n_r-1} & P_{r,n_r} \end{bmatrix}^T$ are the Bezier coefficients. Note that $P_{r,0}$, $P_{r,1}$, P_{r,n_r-1} and P_{r,n_r} are the known coefficients determined by the BCs, and $[X_r]_{(n_r-3)\times 1} = \begin{bmatrix} P_{r,2} & \cdots & P_{r,n_r-2} \end{bmatrix}^T$ are the unknown coefficients that need to be optimized. Matrices $[B_r], [B'_r], [B''_r]$ can be computed using equation (6) and the expressions of $B'_{r,j}(\tau)$ and $B''_{r,j}(\tau)$.[31] Once that the number of Bezier orders and discretization points are given, the matrices are constant matrices. Since this avoids the recomputing of matrices at each iteration, the computation load is effectively reduced.

If $n_r = n_\theta = n_z = 3$, the transfer trajectory is determined analytically by BCs, and there are no unknown coefficients.[31]

If $n_r > 3$, $n_\theta > 3$, and $n_z > 3$, the transfer trajectory cannot be determined analytically by BCs. The unknown coefficients $[X_r]$, $[X_\theta]$, and $[X_z]$ need to be optimized to satisfy certain thrust constraints or achieve some optimal indices. For the time-fixed transfer problem, both the matrices in the Bezier and FFS method are constant matrices when discretization points are given. For the time-free transfer problem, some of the matrices in the FFS method need to be calculated within each iteration.

Using matrix notation, the components of the propulsive acceleration can be expressed in a matrix form referring to equation (1) based on the principle of inverse dynamics

$$\begin{aligned}
[a_r]_{m\times 1} &= a_r\left([r]_{m\times 1}, [z]_{m\times 1}, [\theta']_{m\times 1}, [r'']_{m\times 1}\right) \\
[a_\theta]_{m\times 1} &= a_\theta\left([r]_{m\times 1}, [r']_{m\times 1}, [\theta']_{m\times 1}, [\theta'']_{m\times 1}\right) \\
[a_z]_{m\times 1} &= a_z\left([r]_{m\times 1}, [z]_{m\times 1}, [z'']_{m\times 1}\right)
\end{aligned} \tag{14}$$

and equation (1) is converted to

$$[a] = \sqrt{[a_r]^2 + [a_\theta]^2 + [a_z]^2} \leqslant a_{\max} \tag{15}$$

where $a_{\max}$ is the maximum value of the propulsive acceleration.

In this study, the flight time is an optimization variable. Therefore, the continuous trajectory optimization problem can be transformed into a nonlinear programming problem (NLP)

$$\begin{aligned} &\min_{[X_r],[X_\theta],[X_z],[T]} \quad \Delta V \\ &\text{s.t.} \quad [a] \leqslant a_{\max} \end{aligned} \tag{16}$$

where $[X_r]_{(n_r-3)\times 1}, [X_\theta]_{(n_\theta-3)\times 1}, [X_z]_{(n_z-3)\times 1}$ are the unknown Bezier coefficients of each coordinate. $T \in [T_{\min} \quad T_{\max}]$, $T_{\min}$ is the minimum flight time, and T_{max} is the maximum flight time. The number of variables to be optimized is $n_r + n_\theta + n_z - 8$.

Initialization of unknown coefficients

In this chapter, the initialization method of variables to be optimized is presented. The number of discrete points in the initialization process is n_{APP}. The initialization result is only calculated once as the initial value of the iteration. So in order to make the result more accurate and to not reduce the calculation speed, let $n_{APP} > m$. The flight time T is an optimization variable. The approximated flight time T_{APP} is computed under the following assumptions:

1. The initial and final orbits are circular and coplanar.
2. The spacecraft performs a Hohmann transfer.

Then, by calculating the total ΔV of the Hohmann transfer and considering $a_{\max}$, T_{APP} is obtained as follows

$$T_{APP} = \frac{\left| \sqrt{\frac{\mu_\odot}{r_2}} \left(\sqrt{\frac{2r_1}{r_1+r_2}} \left(1 - \frac{r_2}{r_1}\right) + \sqrt{\frac{r_2}{r_1}} - 1 \right) \right|}{a_{\max}} \times 2 \tag{17}$$

where r_1 and r_2 are the radii of initial and final orbit, respectively. Since the approximated transfer time obtained from the above assumption is far less than the actual time, the result of the above flight time calculation is multiplied by 2.

By using the third-order Bezier curve ($n_r = n_\theta = n_z = 3$), the approximations of r_{APP} can be written as follows (θ_{APP} and z_{APP} have similar structures, see Wall and Conway[20] for details.)

$$\begin{aligned} r_{APP}(\tau) = &(1-\tau)^3 P_{r,0} + 3\tau(1-\tau)^2 P_{r,1} \\ &+ 3\tau^2(1-\tau) P_{r,2} + \tau^3 P_{r,3} \end{aligned} \tag{18}$$

Considering the BCs, these coefficients can be calculated as

$$\begin{aligned} &P_{r,0} = r_i \qquad && P_{r,1} = r_i + T_{APP}\dot{r}_i/3 \\ &P_{r,2} = r_f - T_{APP}\dot{r}_f/3 \qquad && P_{r,3} = r_f \end{aligned} \tag{19}$$

and the scaled time vector is

$$\tau_{App,0} = 0 < \tau_{App,1} < \cdots < \tau_{App,(n_{App}-1)} = 1 \tag{20}$$

Consequently, $[r_{APP}]$ can be obtained by substituting $\tau = \tau_{App}$ into equation (18).

Numerical simulation results

Initial 3D trajectory designs for the exploration of Mars and asteroid Dionysus[28] are carried out to verify the effectiveness of the Bezier method. To verify the superiority of the Bezier method, a comparison with FFS method is also discussed. Moreover, the applicability of the solution obtained by Bezier method is evaluated by introducing the obtained solution into the GPM as an initial guess.[33] Both of the NLPs converted by using Bezier and FFS methods are solved by using the interior point method,[34] and that converted by using GPM is solved by the sequential quadratic programming. All of the test cases are performed on a Intel Core i7 3.40 GHz with Windows 7 and run on MATLAB R2015b.

Earth to Mars

In the FFS method, the number of Fourier terms and discrete points is $n_r = 6, n_\theta = 6, n_z = 4$, $m = 90$, and $n_{APP} = 300$.[28] In the Bezier method, the orders of Bezier curve function and discrete points are $n_r = 12, n_\theta = 12, n_z = 8$, $m = 90$, and $n_{APP} = 300$. Note that the number of unknown coefficients in the Bezier method is $n_r + n_\theta + n_z - 8$, and that in FFS method is $2n_r + 2n_\theta + 2n_z - 8$, therefore there is the same number of unknown coefficients (i.e. 24) in the simulation of the two methods. The maximum propulsive acceleration $a_{\max}$ is set equal to $1.5 \times 10^{-4}\,\text{m/s}^2$,[28] and the departure Julian Day (JD) is 2461102. In the GPM, the number of Legendre-Gauss points is 80. The initial trajectory is

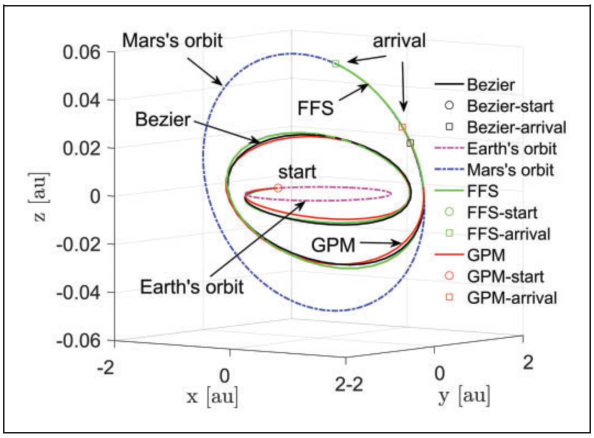

Figure 2. Earth-Mars optimal transfer trajectory with Bezier, FFS, and GPM methods.

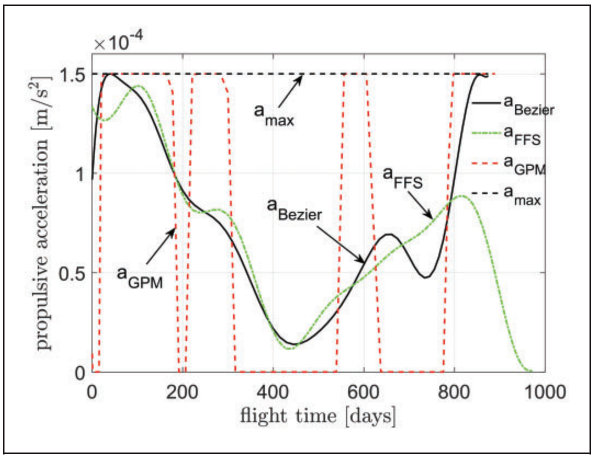

Figure 3. Earth-Mars optimal transfer: time variation of the propulsive acceleration with Bezier, FFS, and GPM methods.

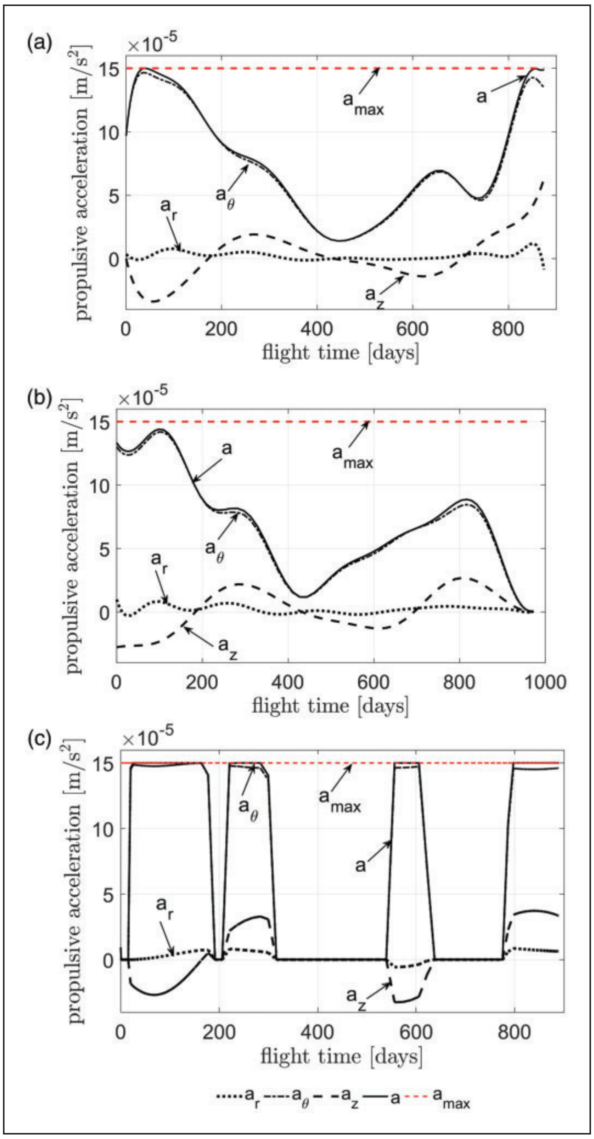

Figure 4. Propulsive acceleration components of Earth-Mars optimal transfer: (a) Bezier, (b) FFS, and (c) GPM.

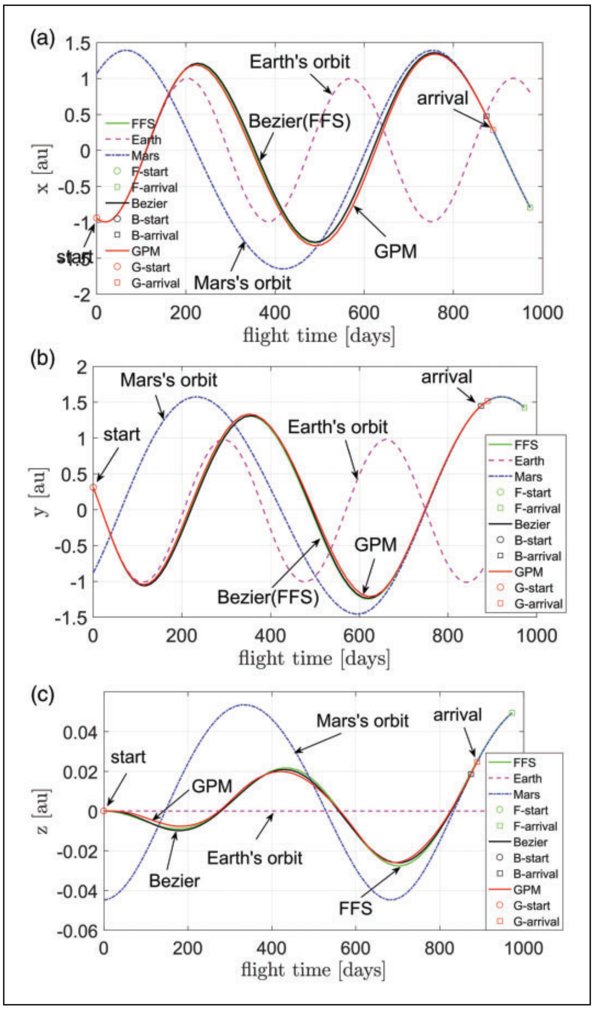

Figure 5. Earth-Mars optimal transfer: time variation of the position vector components with Bezier, FFS, and GPM methods.

designed by using Bezier and FFS method, and the further optimized trajectory is obtained by using GPM, where Bezier provides an initial guess.

Figure 2 shows the optimal transfer trajectory from the Earth to Mars with Bezier, FFS, and GPM methods. The black, green, and red curves represent the results of Bezier, FFS, and GPM methods, respectively. Figure 3 shows the time variation of the propulsive acceleration magnitude obtained using Bezier, FFS, and GPM methods, while Figure 4 shows the propulsive acceleration components computed using the three methods. Figures 5 and 6 show three components of spacecraft position vectors and velocity vectors (heliocentric-ecliptic-inertial system) obtained using the three methods, which are able to meet the BCs very well (the position and velocity errors of the end points are less than the order of 10^{-20}).

The performance index and computation time obtained by the three methods are shown in Table 1. As shown in Table 1, ΔV obtained with the Bezier method is 5.705km/s, and that obtained by FFS and GPM is 5.713 km/s and 5.674 km/s, respectively. The comparison between the Bezier and GPM

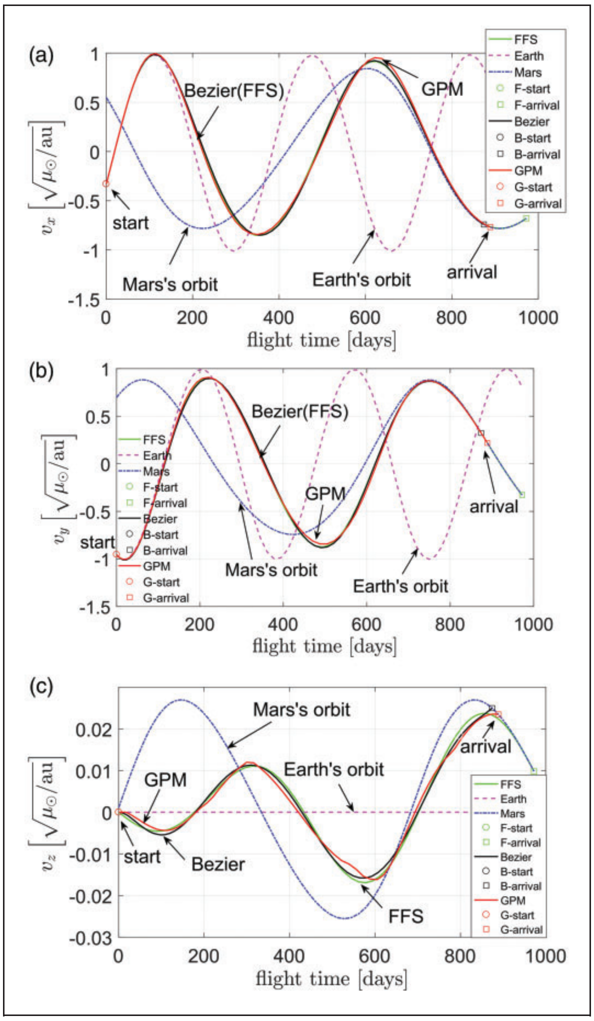

Figure 6. Earth-Mars optimal transfer: time variation of the velocity vector components with Bezier, FFS, and GPM methods.

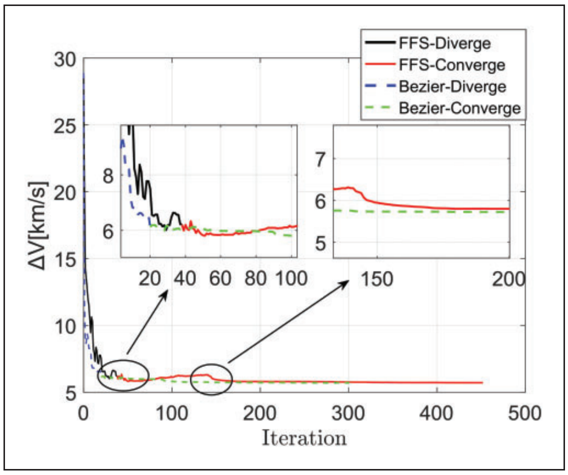

Figure 7. Earth-Mars optimal transfer: comparison of performance index of Bezier and FFS methods with iteration steps.

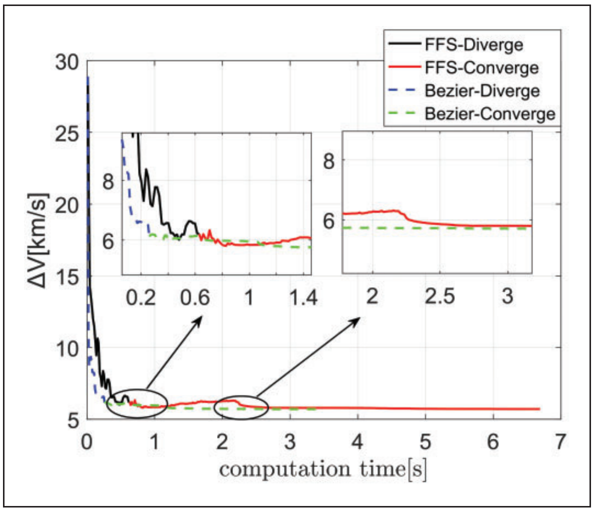

Figure 8. Earth-Mars optimal transfer: comparison of performance index of Bezier and FFS methods with computation time.

Table 1. Earth-Mars optimal transfer: Comparisons of the results of Bezier, FFS, and GPM methods.

Methods	ΔV/(km/s)	Total flight time/(day)	Computation time/(s)
Bezier	5.705	874.26	3.387
FFS	5.713	972.41	6.690
GPM	5.674	889.11	1116.414

results is used to confirm the validity of the Bezier method in the 3D initial trajectory design. In the Earth-Mars example, the difference between performance indices obtained by Bezier and GPM is about only 0.537%. The average computation time used to generate the initial trajectory by using Bezier is 3.387 s, which is about 0.303% of the average computation time used to generate the further optimized trajectory by using GPM.

The comparison between the Bezier and FFS results is used to verify the superiority of the Bezier method. The Bezier method can get better (0.146%) performance-index solution in shorter (50.6%) computation time compared with the FFS method. This is mainly due to the fact that the Bezier method does not need to repeatedly calculate the coefficient matrix in the time-free rendezvous problem. In contrast, some of the matrices in the FFS method need to be calculated within each iteration. Detailed comparison results are shown in Figures 7 to 9. When the simulation converges, the feasible solution satisfying the constraints will be obtained, and then the solution with better performance index will be generated by further iteration until the simulation stops when the change of performance index is less than 10^{-10}. Figure 7 shows the comparison of the performance index of Bezier and FFS methods with iteration steps, from which we can see that the Bezier method can converge with fewer iteration steps and obtain

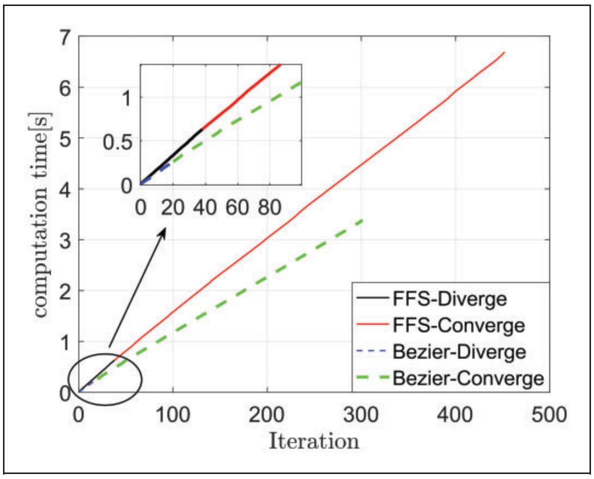

Figure 9. Earth-Mars optimal transfer: comparison of the computational time of Bezier and FFS methods with iteration steps.

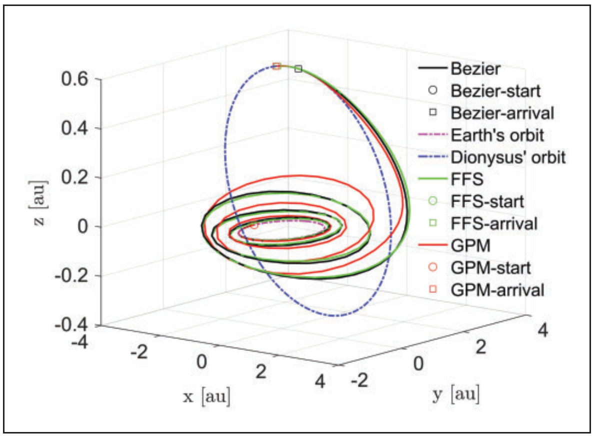

Figure 10. Earth-Dionysus optimal transfer trajectory with Bezier, FFS, and GPM methods.

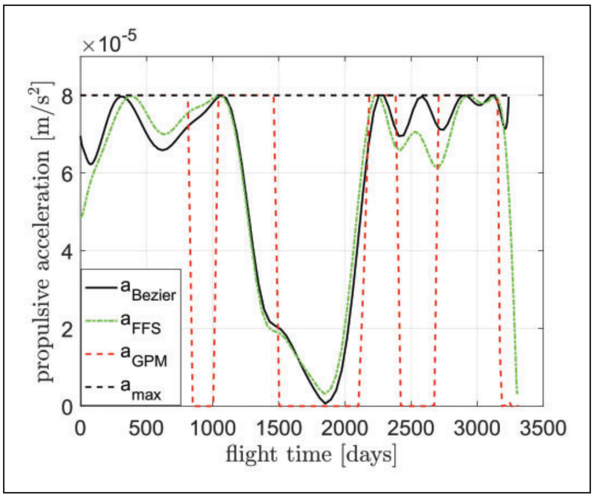

Figure 11. Earth-Dionysus optimal transfer: time variation of the propulsive acceleration with Bezier, FFS, and GPM methods.

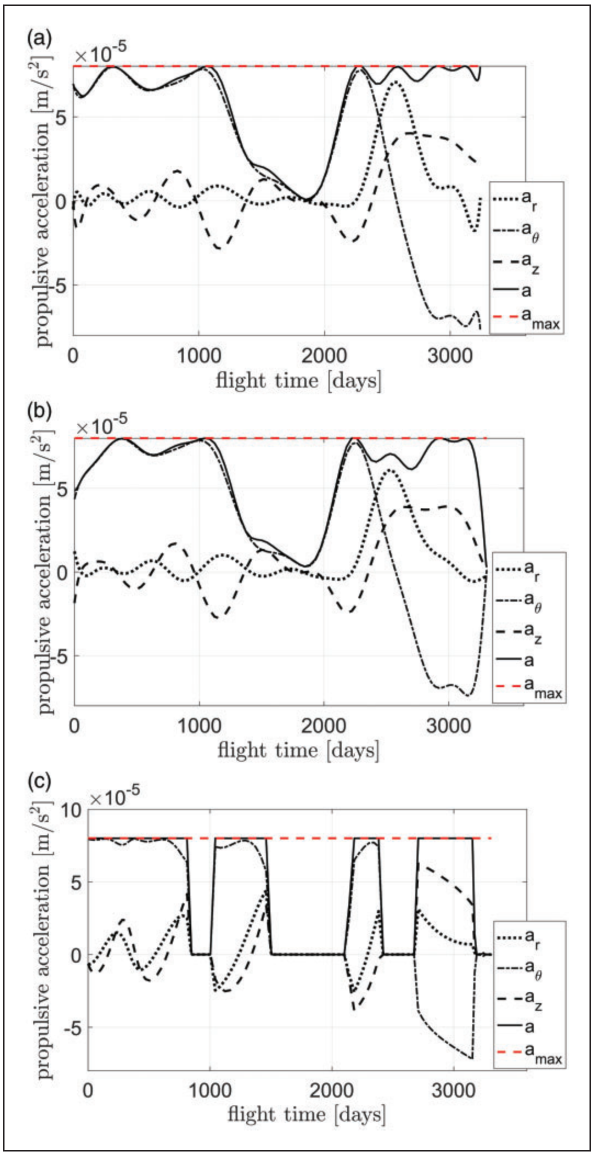

Figure 12. Propulsive acceleration components of Earth-Dionysus optimal transfer: (a) Bezier, (b) FFS, and (c) GPM.

a better performance index. Figure 8 shows the comparison of the performance index of Bezier and FFS methods with computation time, from which we can see that the Bezier method can converge faster and obtain better a performance index. Figure 9 shows the comparison of the computational time of Bezier and FFS methods with iteration steps. It can be seen that the computation time of each iteration of the Bezier method is shorter than that of the FFS method. This also validates the previous analysis. Through the results, we can see that the Bezier method can generate reasonable 3D initial trajectories.

Earth to asteroid Dionysus

In the FFS method, the number of Fourier terms and discrete points are $n_r = 8, n_\theta = 9, n_z = 8, m = 120$, and $n_{APP} = 600$,[28] and while the orders of Bezier curve

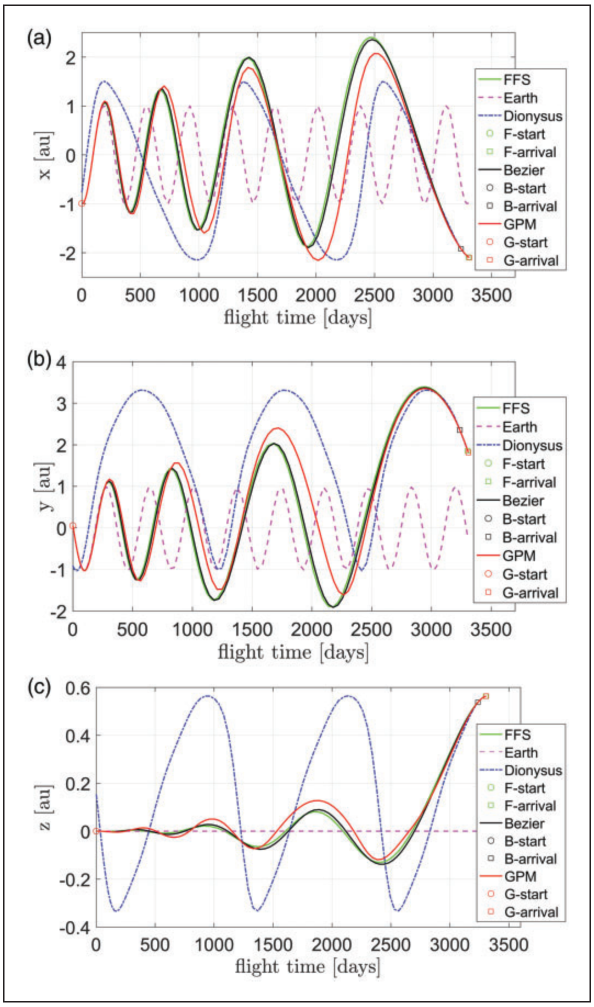

Figure 13. Earth-Dionysus optimal transfer: time variation of the position vector components with Bezier, FFS, and GPM methods.

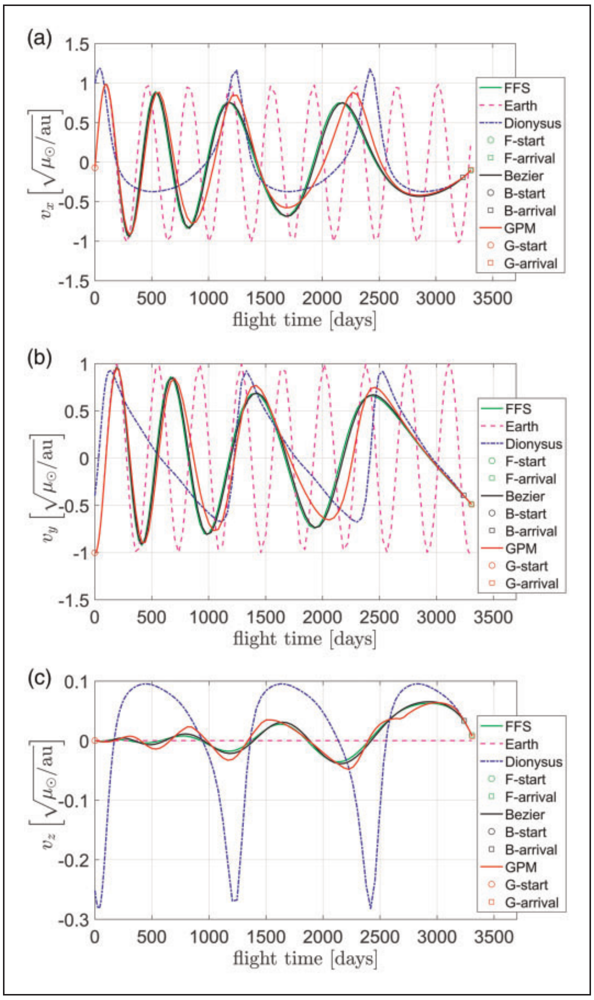

Figure 14. Earth-Dionysus optimal transfer: time variation of the velocity vector components with Bezier, FFS, and GPM methods.

function and discrete points are $n_r = 16$, $n_\theta = 18$, $n_z = 16$, $m = 120$, and $n_{APP} = 600$. The number of unknown coefficients is the same for both the methods. Since the orbital inclination of the asteroid Dionysus is larger and the transfer orbit is more complex, the number of discrete points is higher, in order to get more accurate results. The maximum propulsive acceleration $a_{\max}$ is set equal to $8.0\times 10^{-5}\mathrm{m/s^2}$,[28] and the departure JD is 2458925.5. The initial orbital parameters are taken from Taheri and Abdelkhalik,[28] and the number of revolutions is 5.[28] The number of Legendre-Gauss points of GPM is 120. The initial trajectories are designed by Bezier and FFS methods, and the further optimized trajectory is obtained using GPM, where Bezier provides to it the initial guess.

Figure 10 shows the optimal transfer trajectory from Earth to Dionysus with Bezier, FFS, and GPM methods. The black, green, and red curves represent the results of Bezier, FFS, and GPM methods, respectively. Figure 11 shows the total propulsive acceleration with Bezier, FFS, and GPM methods, and Figure 12 is the thrust acceleration components

Table 2. Earth-Dionysus optimal transfer: Comparisons of the results of Bezier, FFS, and GPM methods.

Methods	ΔV/(km/s)	Total flight time/(day)	Computation time/(s)
Bezier	16.379	3238.41	11.918
FFS	16.392	3304.12	15.868
GPM	11.254	3309.23	1674.3

obtained with the three methods. Figures 13 and 14 show three components of spacecraft position vectors and velocity vectors (heliocentric-ecliptic-inertial system) obtained using the three methods, which is able to meet the BCs very well (the position and velocity errors of the end points are less than the order of 10^{-20} respectively).

The performance index and computation time obtained using the three methods are shown in Table 2. As shown in Table 2, the ΔV obtained by using the Bezier method is 16.379 km/s, and that obtained by using FFS and GPM is 16.392 km/s and 11.254 km/s, respectively. The comparison between

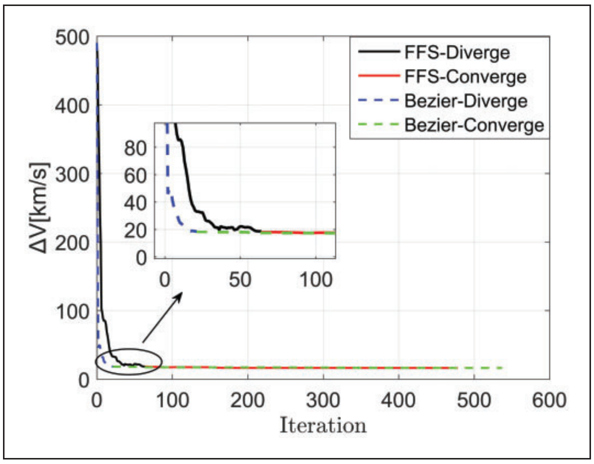

Figure 15. Earth-Dionysus optimal transfer: comparison of performance index of Bezier and FFS methods with iteration steps.

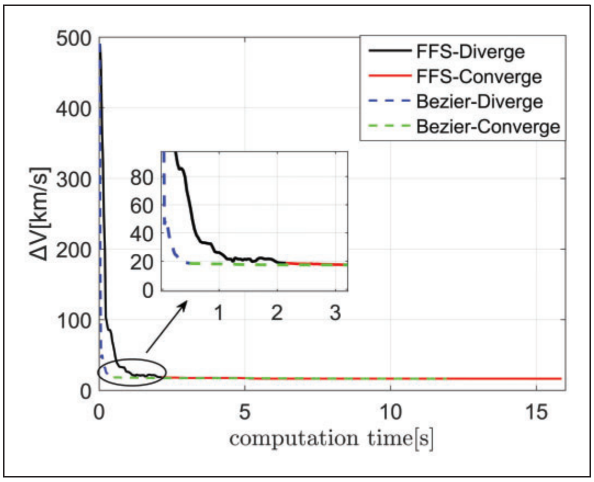

Figure 16. Earth-Dionysus optimal transfer: comparison of performance index of Bezier and FFS methods with computation time.

Bezier and GPM results is used to confirm the validity of the Bezier method in the 3D initial trajectory design of low-thrust transfers. In the Earth-Dionysus example, the difference between the two performance indices obtained using Bezier and GPM is about 31.29%. The average computation time used to generate the initial trajectory by using Bezier is 11.918 s, which is about 0.71% of the average computation time used to generate the further optimized trajectory by using GPM.

The comparison between Bezier and FFS results is used to verify the superiority of the Bezier method. The Bezier method can get better (0.08%) performance-index solution in shorter (75.11%) computation time compared with the FFS method. This is also because the FFS method repeats the calculation of matrices. Figure 15 shows the comparison of the performance indices of Bezier and FFS methods with iteration steps, Figure 16 reports the comparison of

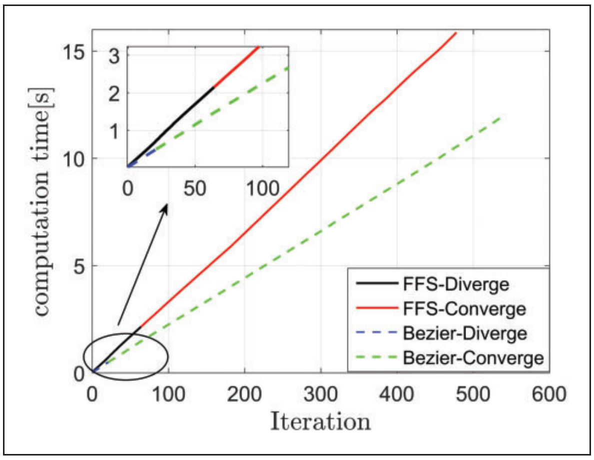

Figure 17. Earth-Dionysus optimal transfer: comparison of the computational time of Bezier and FFS methods with iteration steps.

the performance indices of Bezier and FFS methods with computation time, and Figure 17 shows the comparison of the computational time of Bezier and FFS methods with iteration steps. As can be seen, the Bezier method can converge faster with fewer iteration steps and obtain a better performance index, where the single iteration is faster. This also validates the previous analysis.

From the two examples of Earth-Mars and Earth-Dionysus, compared with the FFS method, the Bezier method can always use shorter computation time to obtain a reasonable 3D initial guess with shorter total flight time and better performance index. The superiority in terms of computational cost is very important for rapid evaluation of the feasibility of a large number of low-thrust flight schemes in the preliminary mission design stage.

Conclusion

In this paper, a novel SB method is proposed by using the Bezier curve to efficiently design three-dimensional low-thrust trajectories. In this method, the orbital coordinates of low-thrust spacecraft are assumed to have the form of Bezier curve function in advance. For the rendezvous problem, the BCs can be satisfied simultaneously by computing 12 coefficients in the Bezier curve function. The EoMs are satisfied by solving a NLP at some Legendre-Gauss distribution of discretization points. In order to verify the superiority of the Bezier method, the comparisons with the FFS method are implemented through numerical simulation. The numerical results show that, for the time-free transfer problem, the Bezier method can get better performance-index solution in shorter computational time compared with the FFS method. This is mainly because the Bezier method does not need to repeatedly calculate the coefficient matrix for time-free rendezvous problem, but some of the matrices in the FFS method need to be calculated within each iteration. The applicability of the solution given by Bezier method is evaluated by introducing the obtained solution into the GPM as an initial guess. The simulation results show that the Bezier method can rapidly generate a very suitable 3D initial trajectory for the optimal solver. This is very important for rapid evaluation of the feasibility of a large number of low-thrust flight schemes in the preliminary mission design stage.

An important part of the method proposed in this paper is the selection of Bezier parameters. This paper is based on the previous references and simulation experiments to determine the number of the corresponding parameters, but the selection of these parameters and the corresponding impact have not been clearly studied, which will be an important research direction in the future.

Declaration of Conflicting Interests

The author(s) declared no potential conflicts of interest with respect to the research, authorship, and/or publication of this article.

Funding

The author(s) disclosed receipt of the following financial support for the research, authorship, and/or publication of this article: This work is supported in part by the National Natural Science Foundation of China under Grant Nos. 11702072 and 11672093, the Innovation Fund of the Shanghai Academy of Spaceflight Technology (SAST) under Grant No. SAST2016039, the China Postdoctoral Science Foundation under Grant No. 2017M611372, the Heilongjiang Postdoctoral Fund under Grant No. LBH-Z16082, and the innovation fund of Harbin Institute of Technology under Grant No. 30620170018.

ORCID iD

Mingying Huo https://orcid.org/0000-0002-7887-3181

References

1. Wang Z and Grant M. Minimum-fuel low-thrust transfers for spacecraft: a convex approach. *IEEE Transac Aerosp Electron Syst* 2018; 54: 2274–2290.
2. Tang G, Jiang F and Li J. Fuel-optimal low-thrust trajectory optimization using indirect method and successive convex programming. *IEEE Transac Aerosp Electron Syst* 2018; 54: 2274–2290.
3. Zhao Z, Shang H, Cui P, et al. Launch opportunity research for Earth-Mars low thrust trajectory. *Proceedings of the 32nd Chinese control conference,* Xi'an, China, 26–28 July. IEEE: Piscataway, NJ, 2013, pp.2350–2355.
4. Xie C, Xu W, Zhang G, et al. Patched shaping approach to low-thrust multi-revolution transfer design. *Proc IMechE, Part G: J Aerospace Engineering* 2019; 233: 2663–2672.
5. Pan B, Pan X and Ma Y. A quadratic homotopy method for fuel-optimal low-thrust trajectory design. *Proc IMechE, Part G: J Aerospace Engineering* 2019; 233: 1741–1757.
6. Shafieenejad I and Novinzadeh AB. Analytical solutions for two-point boundary value problems: optimal low-thrust orbit transfers. *Proc IMechE, Part G: J Aerospace Engineering* 2010; 224: 843–853.
7. Taheri E and Abdelkhalik O. Fast initial trajectory design for low thrust restricted-three-body problems. *J Guidance Control Dyn* 2015; 38: 2146–2160.
8. Sun C, Yuan J and Fang Q. Continuous low thrust trajectory optimization for preliminary design. *Proc IMechE, Part G: J Aerospace Engineering* 2016; 230: 921–933.
9. Petropoulos AE and Sims JA. A review of some exact solutions to the planar equations of motion of a thrusting spacecraft. *2nd international symposium low thrust trajectories*. Toulouse, France, 18–20 June 2002.
10. McConaghy TT, Debban TJ, Petropoulos AE, et al. Design and optimization of low-thrust trajectories with gravity assists. *J Spacecraft Rockets* 2003; 40: 380–387.
11. Izzo D. Lamberts problem for exponential sinusoids. *J Guidance Control Dyn* 2006; 29: 1242–1245.
12. Roa J, Pelaez J and Senent J. New analytic solution with continuous thrust: generalized logarithmic spirals. *J Guidance Control Dyn* 2016; 36: 2336–2351.
13. Wang K and Zhang B. Multiobjective trajectory optimization for a suborbital spaceplane using directed search domain approach. *Aerosp Sci Technol* 2018; 77: 713–724.
14. Zimmer S, Ocampo C and Bishop R. Reducing orbit covariance for continuous thrust spacecraft transfers. *IEEE Transac Aerosp Electron Syst* 2010; 46: 771–791.
15. Novak D and Vasile M. Improved shaping approach to the preliminary design of low-thrust trajectories. *J Guidance Control Dyn* 2011; 34: 128–147.
16. Shafieenejad I, Novinzadeh AB and Molazadeh VR. Introducing a novel algorithm for minimum-time low-thrust orbital transfers with free initial condition. *Proc IMechE, Part G: J Aerospace Engineering* 2015; 229: 333–351.
17. Petropoulos A and Longuski J. Shape-based algorithm for the automated design of low-thrust gravity assist trajectories. *J Spacecraft Rockets* 2004; 41: 787–796.
18. Zhang G and Cao X. Coplanar ground-track adjustment using time difference. *Aerosp Sci Technol* 2016; 48: 21–27.
19. Pascale P and Vasile M. Preliminary design of low-thrust multiple gravity-assist trajectories. *J Apacecraft Rockets* 2006; 43: 1069–1076.
20. Wall B and Conway B. Shape-based approach to low-thrust rendezvous trajectory design. *J Guidance Control Dyn* 2009; 32: 95–101.
21. Wall B. Shape-based approximation method for low-thrust trajectory optimization. *AIAA/AAS astrodynamics specialist conference and exhibit*. Honolulu, Hawaii, 18–21 August 2008, pp.2008–6616.
22. Xie C, Zhang G and Zhang Y. Simple shaping approximation for low-thrust trajectories between coplanar elliptical orbits. *J Guidance Control Dyn* 2015; 38: 2448–2455.
23. Xie C, Zhang G and Zhang Y. Shaping approximation for low-thrust trajectories with large out-of-plane motion. *J Guidance Control Dyn* 2016; 39: 2776–2786.

24. Gondelach DJ and Noomen R. Hodographic-shaping method for low-thrust interplanetary trajectory design. *J Spacecraft Rockets* 2015; 52: 728–738.
25. Zeng K, Geng Y and Wu B. Shape-based analytic safe trajectory design for spacecraft equipped with low-thrust engines. *Aerosp Sci Technol* 2017; 62: 87–97.
26. Peloni A, Dachwald B and Ceriotti M. Multiple near-earth asteroid rendezvous mission: solar-sailing options. *Adv Sp Res* 2018; 62: 2084–2098.
27. Abdelkhalik O and Taheri E. Approximate on-off low-thrust space trajectories using Fourier series. *J Spacecraft Rockets* 2012; 49: 962–965.
28. Taheri E and Abdelkhalik O. Initial three-dimensional low-thrust trajectory design. *Adv Sp Res* 2016; 57: 889–903.
29. Taheri E, Kolmanovsky I and Atkins E. Shaping low-thrust trajectories with thrust-handling feature. *Adv Sp Res* 2018; 61: 879–890.
30. Huo M, Zhang G, Qi N, et al. Initial trajectory design of electric solar wind sail based on finite Fourier series shape-based method. *IEEE Transac Aerosp Electron Syst* 2019; 55: 3674–3683.
31. Huo M, Mengali G, Quarta A, et al. Electric sail trajectory design with Bezier curve-based shaping approach. *Aerosp Sci Technol* 2019; 88: 126–135.
32. Janhunen P. Electric sail for spacecraft propulsion. *J Propul Power* 2004; 20: 763–764.
33. Benson D. *A gauss pseudospectral transcription for optimal control*. PhD Thesis, MA Institute of Technology, Cambridge, 2005.
34. Jiang F. Pseudospectral methods for trajectory optimization with interior point constraints: verification and applications. *IEEE Transac Aerosp Electron Syst* 2005; 49: 2005–2017.